

Structure and photoluminescence of ZnSe nanoribbons grown by metal organic chemical vapor deposition

X. T. Zhang, K. M. Ip, Z. Liu, Y. P. Leung, Quan Li, and S. K. Hark^{a)}

Department of Physics, The Chinese University of Hong Kong, Shatin, Hong Kong

(Received 8 September 2003; accepted 6 February 2004)

ZnSe nanoribbons have been synthesized using sputter-coated gold films as catalysts via metalorganic chemical vapor deposition on Si (100) substrates. Both x-ray and selected area electron diffractions determine that they have the zinc-blende structure. High-resolution transmission electron microscopic investigations show that their structure is highly ordered and contains coherent twin lamellae near one edge but is essentially free of dislocations. Photoluminescence studies at 10 K show that sharp excitonic peaks dominate their spectra, reflecting their high purity and nearly perfect stoichiometry. New excitonic peaks are observed in the nanoribbons and their possible origins are discussed. © 2004 American Institute of Physics. [DOI: 10.1063/1.1695096]

Quasi-one-dimensional (1D) nanometer-sized semiconductor structures in the forms of nanowires, nanorods, and nanoribbons have attracted considerable interest because of their usefulness as elementary building blocks in nanotechnology¹ and potential applications in optoelectronic nanodevices. Recently, the growths of group IV, III–V, and II–VI 1D semiconductor nanostructures have been achieved by various methods.² However, a large portion of the work on II–VI quasi-1D systems has focused on ZnO, ZnS, CdSe, and CdS. Only a few studies on ZnSe were reported,^{3–5} although there exists an extensive literature on the growth of other ZnSe nanostructures, such as epitaxial layers,⁶ quantum wells,⁷ and quantum dots.⁸ As far as we know, growing ZnSe 1D nanostructures by metalorganic chemical vapor deposition (MOCVD) has not been reported, although such growths of III–V nanowires have been reported.⁹ In this letter, we report the success in using gold as a catalyst to synthesize ZnSe nanoribbons on Si (001) substrates by MOCVD, a technique of demonstrated value in the commercial production of blue-green light emitting devices.

The conditions of MOCVD growth were reported elsewhere.¹⁰ The synthesized products were characterized by x-ray diffraction (XRD) using the Cu K α radiation, scanning electron microscope (SEM), high-resolution transmission electron microscope (TEM), atomic force microscope (AFM), and photoluminescence (PL) spectroscopy.

The SEM image of Fig. 1(a) shows that the synthesized product consists of a high density of long nanoribbons, whose lengths range from several to tens of micrometers. The x-ray diffraction (XRD) pattern of the nanoribbons is shown in Fig. 1(b). All of the diffraction peaks can be indexed to a zinc-blende-structured ZnSe. Their ribbon like shape is confirmed by TEM and AFM. An AFM image of a typical nanoribbon, having a width of about 210 nm and thickness 30 nm, is shown in Fig. 2(a). TEM observations of two nanoribbons are shown in Fig. 2(b). The lattice-resolved image of Fig. 2(c) clearly reveals the {111} atomic planes and the $\langle 112 \rangle$ direction of growth. Stacking faults and twin lamel-

lae are seen running along the length and only near one edge of the flat nanoribbon. Since these defects are not randomly distributed within, the structure of the nanoribbons remains largely coherent. Moreover, we should remark that because they appear to terminate at the surfaces and not bounded by partial dislocations within the nanoribbons, they are not electrically active and do not create a local electric or strain field. As such, their presence does not inhibit the formation and recombination of excitons.

For cubic crystals to display 1D growth habits, certain symmetry breaking mechanism is required to account for the

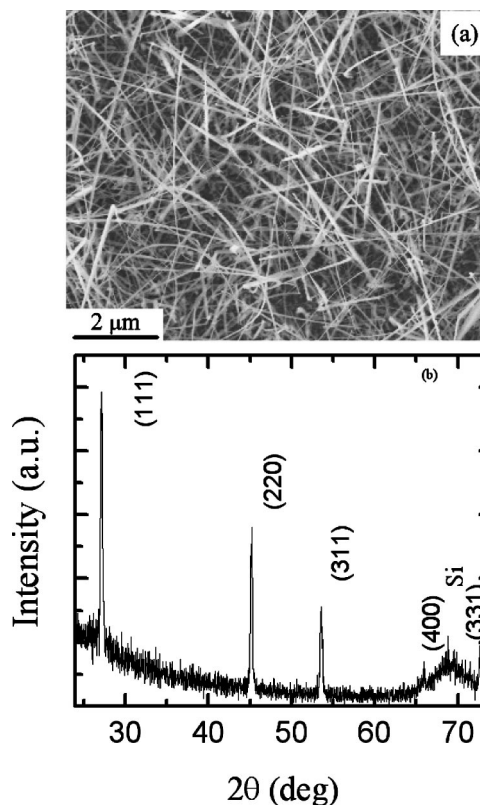


FIG. 1. (a) A typical SEM image of the synthesized products; (b) XRD pattern of the synthesized products; the broad peak at 68° is from the substrate, Si (004).

^{a)}Author to whom correspondence should be addressed; electronic mail: skhark@phy.cuhk.edu.hk

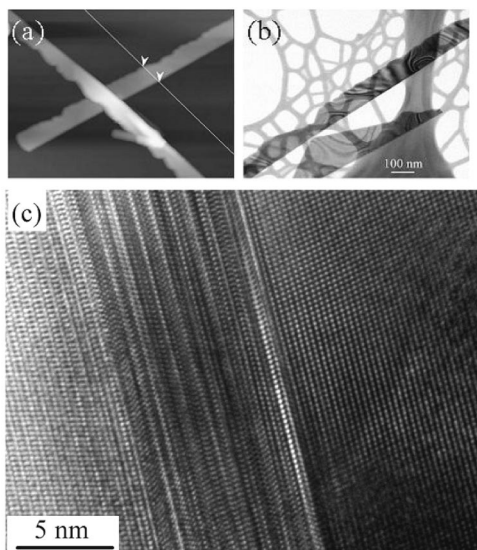


FIG. 2. Microscopic images of ZnSe nanoribbons: (a) AFM image showing two cross overlapped flat nanoribbons with a saw-tooth edge; a short nanowire is also seen; the line and the arrow heads indicate where the profile of the nanoribbon was traced. (b) TEM image of another two nanoribbons that are partially transparent. (c) HRTEM image showing the $\{111\}$ planes and the coherent twin lamellae structure within.

large anisotropy. Many such mechanisms have been proposed, two of the better-known ones are found in the VLS and emergent dislocation models. For the effective operation of the VLS mechanism, the presence of a particle at the tip is necessary. However, a particle of Au alloy has never been found at the tip of the vast number of nanoribbons studied by TEM and AFM. Moreover, our nanoribbons were grown at 550°C , a temperature far too low for Au to melt, even when particle size depression of the melting point is considered.¹¹ More important, the $\langle 112 \rangle$ growth direction also lends support in ruling out VLS. Rapid crystal growth along one direction requires a self-perpetuating growth site. An emergent screw dislocation could provide the required site but it could not explain the preferred $\langle 112 \rangle$ growth direction. Instead of growth spirals or screw dislocations, we found only stacking faults and twin lamellae. It has been shown that these can also provide self-perpetuating growth sites in fcc crystals in the form of reentrant corners.^{12,13} Under high supersaturation, growth via the reentrant corner mechanism is faster than even the emergent screw dislocation mechanism.^{14,15} Whisker growth along the $\langle 112 \rangle$ direction by the reentrant angle mechanism has been confirmed in Si and Ge. In these whiskers the resulting morphology is similar to our ZnSe nanoribbons, in that the growth direction is $\langle 112 \rangle$ and the major terminating surfaces are the $\{111\}$ and $\{110\}$ planes.¹⁵ We believe the Au particles probably act as the nucleating sites for ZnSe embryos, as nanoribbons tend not to grow without them.

Figure 3 shows the PL spectra of the nanoribbons at 10 and 298 K. The sharp peaks I_2 and I_1 are readily attributed to bound excitons. From the energy of the band gap (2.820 eV) and that of the band to acceptor (BA) peak, the acceptor binding energy is deduced to be 70 meV.¹⁶ The barely resolved doublet at 2.721 eV is attributed to emissions from donor-acceptor pair transitions. The donor is suggested to be Ga_{Zn} and acceptor As_{Se} . Not only do these identifications

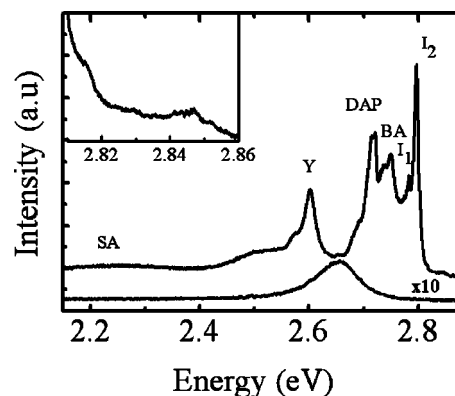


FIG. 3. PL spectra of the ZnSe nanoribbons at room temperature and at 10 K. The photon energies in eV are I_2 (2.798), I_1 (2.784), BA (2.750). The inset shows the new above band gap peak.

agree with the accepted ionization energies¹⁷ of the impurities, they can also be traced to a plausible source within our MOCVD growth chamber, which was also used to grow other nanostructures on GaAs substrates. Sublimation of GaAs is known to occur at 550°C , the growth temperature of the nanoribbons,¹⁸ and might have resulted in unintentional doping by cross-contamination. The peak at 2.602 eV is the Y-line luminescence, which has been linked to the presence of structural defects in materials of low impurity concentration.¹⁹ The weak deep-level emissions, possibly involving self-activated defects centered around 2.3 eV, indicate the nearly perfect stoichiometric composition of the nanoribbons.²⁰ The bound exciton peaks are slightly broadened (~ 10 meV), possibly caused by the proximity of the complexes to the surface of the nanoribbons, which was not intentionally passivated. The broadened I_2 peak also obscures the observation of free excitons. At higher photon energies (Fig. 3, inset), we note the existence of two small peaks at 2.849 and 2.816 eV. The former is new, seen for the first time in zinc-blende-structured ZnSe; its energy is some 29 meV above the band gap. Its energy coincides with the bound exciton emissions in wurtzite-structured ZnSe.²¹ However, our XRD results and TEM studies found only zinc-blende-structured ZnSe. The origin of this peak can be understood if we assign it to excitons bound to impurities located within the twin lamellae region of the nanoribbons. Since their Bohr radius is small (~ 40 Å), the excitons only see the local hexagonal environment. Were it not for the coherent nature of the twin lamellae and the quasi-1D nature of the nanoribbons, the excitons would not have formed and their emissions been able to escape outside. In three-dimensional or even quasi-two dimensional structures, stacking faults and twin lamellae are usually bounded by partial dislocations, whose associated local space charges would field-ionize most of the weakly bound excitons. Moreover, the surrounding zinc-blende materials would absorb any above band gap photons from the surviving excitons, except those emitting very near the surface. The nanoribbons, on the other hand, naturally provide many nearby exit surfaces. There are two possible assignments for the peak at 2.816 eV. Energy considerations alone would suggest it is either from the first excited state of free excitons or a LO-phonon replica of the 2.845 eV peak. In view of its intensity and the fact that there is no evidence of a peak or a shoulder that could be

assigned to the free exciton ground state, we favor the latter assignment. Its intensity is comparable to the zero phonon emission only because the latter is partially absorbed. At room temperature, only the significantly thermal broadened band edge emission at 2.67 eV survives, indicating the essentially defect free nature of MOCVD grown nanoribbons. Using catalysts has often been a concern in the growth of nanowires and nanoribbons, because of the possibility of doping. Au has not been found as a likely source of impurity in our MOCVD growth of ZnSe, perhaps because of the low temperature involved.

In conclusion, long, highly ordered zinc-blende-structured ZnSe nanoribbons were successfully grown on Si (001) substrate sputtered-coated with a thin film of Au at low temperatures for the first time by MOCVD. Au, as a catalyst, does not lead to VLS growth and contamination, but acts as a nucleating site for ZnSe embryos containing stacking faults and twin lamellae, which were identified within the nanoribbons. These faults, however, do not have any apparent detrimental effects on the photoluminescence properties of the nanoribbons. In fact, new excitonic emissions are identified to be associated with them.

The work in this letter, was partially supported by grants from the Research Grants Council of the Hong Kong Special Administrative Region, China (Project No. CUHK 4247/01P) and CUHK Direct Grant (Project Code No. 2060238).

- ¹C. M. Lieber, *Solid State Commun.* **107**, 607 (1998).
- ²Y. Xia, P. Yang, Y. Sun, Y. Wu, B. Mayers, B. Gates, Y. Yin, F. Kim, and H. Yan, *Adv. Mater. (Weinheim, Ger.)* **15**, 353 (2003).
- ³W. Z. Wang, Y. Geng, P. Yan, F. Y. Liu, Y. Xie, and Y. T. Qian, *Inorg. Chem. Commun.* **2**, 83 (1999).
- ⁴N. Kouklin, L. Menon, and S. Bandyopadhyay, *Appl. Phys. Lett.* **80**, 1649 (2002).
- ⁵H. P. Wagner, W. Langbein, J. M. Hvam, G. Bacher, T. Kümmell, and A. Forchel, *Phys. Rev. B* **57**, 1797, (1998).
- ⁶X. B. Zhang, K. L. Ha, and S. K. Hark, *Appl. Phys. Lett.* **79**, 1127 (2001).
- ⁷H. Tho, H. E. Jackson, S. Lee, M. Dobrowolska, and J. K. Furdyna, *Phys. Rev. B* **61**, 15641 (2000).
- ⁸D. Sarigiannis, J. D. Peck, G. Kioseoglou, A. Petrou, and T. J. Mountziaris, *Appl. Phys. Lett.* **80**, 4024 (2002).
- ⁹M. Yazawa, M. Koguchi, A. Muto, M. Ozawa, and K. Hiruma, *Appl. Phys. Lett.* **61**, 2051, (1992).
- ¹⁰X. T. Zhang, Z. Liu, Y. P. Leung, Q. Li, and S. K. Hark, *Appl. Phys. Lett.* **83**, 5533 (2003).
- ¹¹Y. G. Chushak and L. S. Bartell, *J. Phys. Chem. B* **105**, 11605 (2001).
- ¹²A. I. Bennett and R. L. Longini, *Phys. Rev.* **116**, 53 (1959).
- ¹³R. S. Wagner and R. G. Treuting, *J. Appl. Phys.* **32**, 2490 (1961).
- ¹⁴H. Li, X. D. Peng, and N. B. Ming, *J. Cryst. Growth* **149**, 24 (1995).
- ¹⁵N. B. Ming, K. Tsukamoto, I. Sunagawa, and A. A. Chernov, *J. Cryst. Growth* **91**, 11 (1988).
- ¹⁶J. Gutowski, N. Presser, and G. Kudler, *Phys. Status Solidi A* **120**, 11 (1990).
- ¹⁷P. J. Dean, D. C. Herbert, C. J. Werkhoven, B. J. Fitzpatrick, and R. N. Bhargava, *Phys. Rev. B* **23**, 4888 (1981).
- ¹⁸A. Guillen-Cervantes, Z. Rivera-Avarez, M. Lopez-Lopez, E. Lopez-Luna, and I. Henandez-Calderon, *Thin Solid Films* **373**, 159 (2000).
- ¹⁹K. Shahzad, J. Petruzzello, D. J. Olego, D. A. Cammack, and J. M. Gaines, *Appl. Phys. Lett.* **57**, 2452 (1990).
- ²⁰J. W. Allan, *Semicond. Sci. Technol.* **10**, 1049 (1995).
- ²¹W. Y. Liang and A. D. Yoffe, *Philos. Mag.* **16**, 1153 (1967).